

## New method for full field measurement of pore water pressures

Broere, Wout; Dijkstra, J.; Ottolini, M

**DOI**

[10.1201/9780429438660-43](https://doi.org/10.1201/9780429438660-43)

**Publication date**

2018

**Document Version**

Final published version

**Published in**

Physical Modelling in Geotechnics

**Citation (APA)**

Broere, W., Dijkstra, J., & Ottolini, M. (2018). New method for full field measurement of pore water pressures. In A. McNamara, S. Divall, R. Goodey, N. Taylor, S. Stallebrass, & J. Panchal (Eds.), *Physical Modelling in Geotechnics* (pp. 323–327). Taylor & Francis. <https://doi.org/10.1201/9780429438660-43>

**Important note**

To cite this publication, please use the final published version (if applicable). Please check the document version above.

**Copyright**

Other than for strictly personal use, it is not permitted to download, forward or distribute the text or part of it, without the consent of the author(s) and/or copyright holder(s), unless the work is under an open content license such as Creative Commons.

**Takedown policy**

Please contact us and provide details if you believe this document breaches copyrights. We will remove access to the work immediately and investigate your claim.

***Green Open Access added to TU Delft Institutional Repository***

***'You share, we take care!' - Taverne project***

**<https://www.openaccess.nl/en/you-share-we-take-care>**

Otherwise as indicated in the copyright section: the publisher is the copyright holder of this work and the author uses the Dutch legislation to make this work public.

## Development of an instrumented model pile

A.B. Lundberg

*Geotechnical Department, ELU Konsult AB, Stockholm, Sweden*

W. Broere

*Geo-engineering Section, Delft University of Technology, Delft, The Netherlands*

J. Dijkstra

*Division of Geology & Geotechnics, Chalmers University of Technology, Gothenburg, Sweden*

**ABSTRACT:** An instrumented model pile has been realized to study the displacement pile installation effects in sand in physical model tests. The system includes a model pile, instrumented with axial and horizontal contact stress sensors, and a corresponding calibration apparatus. The development of the instrumented model pile, including numerical analysis of the mechanical response during testing, and an optimization of the instrumentation to minimize thermal effects are described. The performance of this new model pile is demonstrated using calibration measurements and an example application in a physical model test at an elevated stress level in the geotechnical centrifuge.

### 1 INTRODUCTION

The axial bearing capacity of piles consists of the base resistance and the shaft resistance. For long piles in sand, the shaft resistance governs the total bearing capacity, (Klotz and Coop 2001, Randolph et al. 1994). In turn, the pile shaft resistance results from the sum of local shaft friction along the pile. In sands the local shaft friction is approximated in terms of Coulomb friction (Lehane et al. 1993), controlled by the effective horizontal contact stress at the pile-soil surface at the depth  $z$  and the interface friction. The interface friction angle is possible to obtain from laboratory tests, (Jardine et al. 1993), while the horizontal contact stress consists of the effective normal stress at the pile surface, i.e. the lateral stress in the subsoil. The horizontal contact stress is difficult to obtain in-situ, even from instrumented pile load tests, with some exceptions where highly controlled field test set-ups have been conceived, (Lehane et al. 1993, Jardine et al. 2013). The installation of displacement piles results in large disturbances of the initial soil state, i.e. the stress and density, due to the large soil deformations, (Poulos and Davis 1980, Jardine et al. 2013). The distribution of the horizontal contact stress  $\sigma_n(z)$  along the pile shaft and consequently the pile bearing capacity is therefore highly influenced by the installation, resulting in significant differences in the load-displacement response of displacement piles compared to bored piles, where different installation effects have occurred, (Poulos and Davis 1980). Prediction methods for the axial pile bearing capacity have

consequently relatively low accuracy, since the soil state after installation needs to be assessed based on the initial site investigation data, (Randolph et al. 1994). The bearing capacity and load-deformation response of a pile group is even more complicated to assess, due to the interaction between piles during installation, (Stuedlein and Gianella 2016). A more thorough comprehension of the pile installation process would therefore be of practical use.

Experimental research in which the normal stress  $\sigma_n(z)$  acting on the pile is measured is required to arrive at an accurate description of the governing mechanisms of pile shaft friction. Due to the change in soil state during pile installation shown in (Lehane et al. 1993), local measurements are necessary to properly study the evolution of horizontal normal stress during the installation process. A measurement system has therefore been developed to locally measure soil horizontal normal stress  $\sigma_n(z)$  on a continuous model pile surface. This system includes the design and instrumentation of an instrumented model pile, as well as a calibration system in which both normal stress sensors and axial stress sensors were calibrated. The design of the normal stress sensors was a compromise between the stress sensor sensitivity and minimization of influence from the axial load in the pile. The latter effect had been observed in other types of stress measurements as well, e.g. (Klotz and Coop 2001).

There are various methods to measure the local contact stress. These include surface sensors located on a structure (El Ganainy et al. 2013, Talesnick et al. 2014), and embedment cells surrounding the

pile, (Foray et al. 1993, Jardine et al. 2013). Embedment cells require large soil models for instrumentation space, and are therefore not very suitable in the geotechnical centrifuge. The spatial accuracy of a small number of such cells is relatively low, as concluded by (Foray et al. 1993). Normal stress transducers mounted on the pile surface were therefore included in the instrumented model pile to measure the horizontal normal stress. Laboratory measurements show influence of grain size, stress distribution, hysteresis and sensor stiffness, (Talesnick et al. 2014). The soil grain size does not scale in centrifuge model tests (Garnier et al. 2007), therefore the soil grains are relatively large in relation to the stress sensor. Possible arching mechanisms redistribute the normal stress at the sensor, especially for external earth pressure cells mounted on the surface of a structure, (Foray et al. 1993). Installation of external earth pressure cells also result in a variation in pile surface roughness, e.g. as reported by (Klotz and Coop 2001). Especially, during cyclic shear loading, these effects redistribute the stress around the sensor (Randolph et al. 1994). A membrane strain gauge configuration directly embedded in the pile wall was therefore chosen for the current model pile to minimize the effect of stress redistribution. The membrane strain gauge consists of a flexible diaphragm on which a strain gauge bridge is mounted. In a novel configuration the flexible diaphragm is the pile surface itself, which deflects from the external soil pressure. As opposed to the null sensor (Talesnick et al. 2014), the membrane deflects under loading and the load is directly inferred from the membrane deflection rather than from a compensating fluid pressure. By omitting the null-sensor concept allows for extensive instrumentation on a relatively small model pile for the geotechnical centrifuge at the expense of allowing for movement in the soil that might affect the readings.

## 2 MECHANICAL DESIGN

The mechanical design of one half of the model pile is shown in Figure 2. The  $125 \times 10 \times 10 \text{ mm}^3$  instrumented pile was assembled from two identical milled steel sections. The model pile after assemblage is shown in Figure 1. The half bridge was mounted on the flexible membrane at cross-section A, shown to the right in Figure 2. The layout of the membrane was designed using analytical and numerical methods. The upper bound of the horizontal normal stresses, governing the membrane thickness, was estimated from available published data at 300-500 kPa (Boulon and Foray 1986, Foray et al. 1993, Lehane et al. 1993, Jardine et al. 2013). The membrane width was set to 8 mm, and the cross-section thickness  $h$  calculated from analytical formulas for a clamped circular plate (Reddy 2006):

$$\varepsilon_{rr} = \frac{3p(1-\nu^2)}{8Eh^2}(a-3r^2) \quad (1)$$

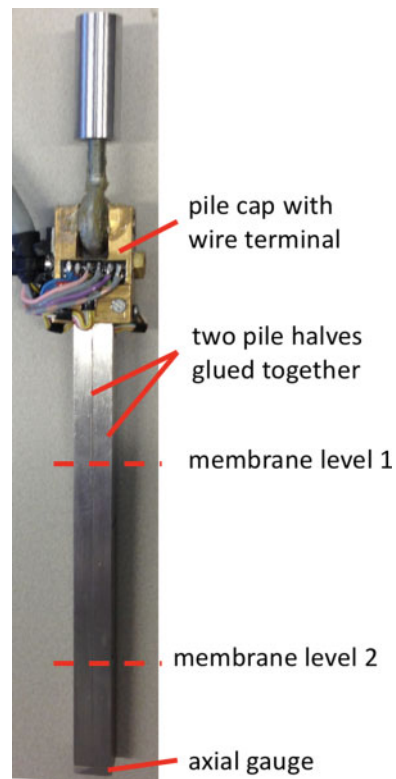


Figure 1. Image of the model pile.

Where  $E$  is the elastic modulus of the steel,  $p$  is the normal stress,  $h$  is the membrane thickness,  $a$  is the membrane radius,  $r$  is the position in the radial direction and  $\nu$  is the Poisson's ratio. The maximum strain occurs in the middle of the membrane. This resulted in a membrane thickness of 0.3 mm for our geometry and material (stainless steel: Young's modulus  $E$  of 210 GPa and Poisson's ratio  $\nu$  of 0.29).

Further analysis was carried out with the 3D-Finite Element program COMSOL Multiphysics version 4.3, (Comsol 2008). Ten-noded tetrahedral elements and triangular surface elements were used in the model to mesh the pile. The numerical model offered the possibility to model the influence of combined horizontal contact stress and pile axial load, which naturally would occur during the model tests. First the effect of variation in fabrication tolerance was studied by varying the membrane thickness to 0.27 mm, 0.29 mm, 0.31 mm, and 0.33 mm. The model pile was simulated loaded in the axial and in the horizontal normal direction at the pile surface, and the strain  $\varepsilon_{yy}$  perpendicular to the pile axis at the location of the stress sensors was obtained from the numerical model. The simulations were normalized with the strain level for the design dimension,  $\varepsilon_{yy,30}$ . The results demonstrate a  $\pm 27\%$  deviation in sensitivity for horizontal contact stress and a  $\pm 8\%$  sensitivity for axial load for each  $\pm 10\%$  successive change in the membrane thickness. After manufacturing of the membranes the tolerances in

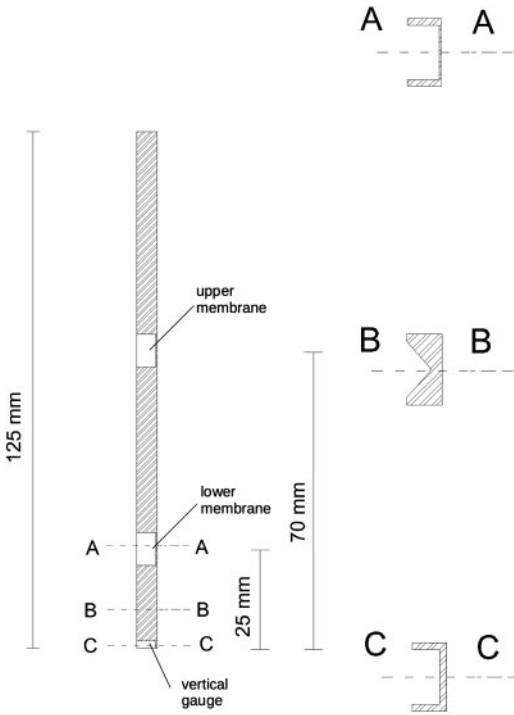
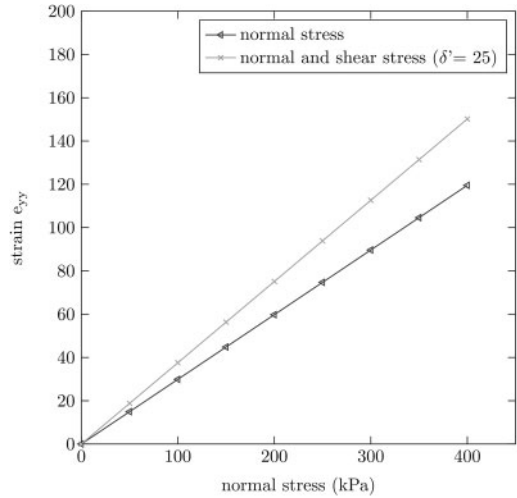


Figure 2. Details of model pile.

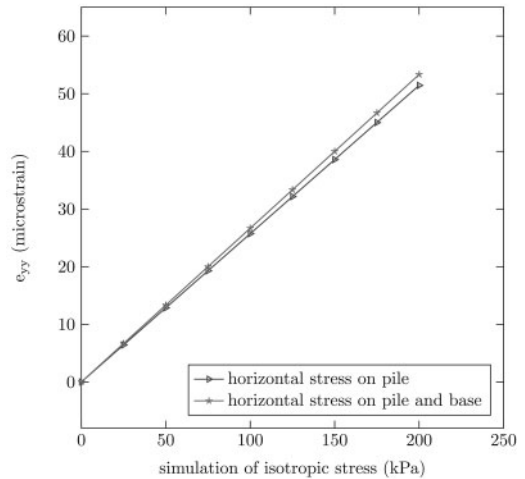
thickness were found to be  $< 5\%$ . Therefore, the sensitivity of the sensor is within a reasonable bandwidth for the data acquisition equipment and easily accounted for in the calibration.

During installation the pile is subjected to both normal and shear strain at the pile shaft. The effect of shear stress on the membrane surface was simulated with the numerical model with a coefficient of friction  $\mu = 0.466$ , corresponding to an interface friction angle  $\delta = 25^\circ$ , which is a reasonable assessment of common field and laboratory pile-soil conditions according to (Jardine et al. 1993). The simulation result is shown in Figure 3, which shows an increase in horizontal strain level  $\varepsilon_{yy}$  of around 25% at fully mobilized shear load.

Finally, a calibration of the horizontal normal stress sensor system in a pressure vessel was numerically simulated by application of an isotropic stress around the pile. The isotropic stress also resulted in axial stress component in the pile that loads the membranes axially. The extra horizontal strain  $\varepsilon_{yy}$  from combined axial and horizontal normal loading during isotropic calibration of the model pile is shown in Figure 3. The additional axial component leads to a higher horizontal strain level. This requires a correction of the measurements and resulting calibration factors for the horizontal contact stress sensors for the axial load. The numerical simulations lead to adopting a factor  $R_{axial} = 0.963$ , which was multiplied by the calibration measurements to retrieve the correct values of the calibration coefficients.



(a) The effect of shear stress on the membrane.



(b) Axial load effects.

Figure 3. The effect of additional shear stress and axial load in model pile on the contact stress gauge.

### 3 INSTRUMENTATION SYSTEM

#### 3.1 Pile instrumentation

The model pile instrumentation system consisted of four horizontal contact stress sensors and one axial stress sensor located near the base of the pile. The horizontal contact stress sensors comprise a strain gauge half-bridge. The half strain gauge bridge consisted of two  $120\Omega$  strain gauges and two  $120\Omega$   $0.1\%$   $5\text{ppm}/^\circ\text{C}$  high precision SMD resistors. The strain gauge excitation voltage was  $6\text{V}$ , which was supplied by the in-flight amplifier system on the geotechnical centrifuge. The  $120\Omega$  strain gauges were of the

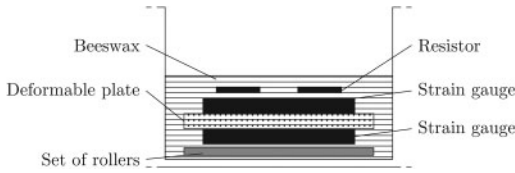


Figure 4. Detail of strain gauge configuration on membrane gauge (located at the bottom), not to scale. Rollers are 0.5 mm graphite pencil stifts.

type TML FLA 2-11, and had a tolerance of 0.1%, and a temperature compensation for steel of ( $11 \cdot 10^{-6} \text{ m/mK}$ ).

The two strain gauges were mounted on each side of a thin flexible plate, shown in Figure 4. The electrical configuration is such that only bending is picked up by the strain-gauges. Axial load in the plate is automatically compensated for. This plate could therefore be glued in the cavity to operate invariant of detrimental effects from axial loads. Also, shear stress in the membrane itself is compensated for by placing this ‘bending-plate’ at a distance from the membrane and only in contact to the membrane with small 0.5 mm graphite rods. As a result only the additional bending resulting from the axial loads are still influencing the measurements. The latter is compensated for by extensive calibration for load combinations supported by the numerical analysis of the pile, which has been previously discussed. The resistors, complementing the strain gauge bridge, were installed on top of the bending-plate with the strain gauges, before being covered with beeswax. The axial stress sensor consisted of two strain gauges placed opposite each other in a half Wheatstone bridge configuration and are mounted at opposite internal sides in the model pile. This electrical configuration doubles the sensitivity in axial direction and compensates for bending, however only in one direction, in this case the more compliant. The sensitivity of all the strain gauge bridges were optimized for an amplification of 1000x in the custom designed strain gauge amplifier such that no additional digital gain on the National instruments PCI-6220 acquisition card was required.

### 3.2 Excitation and data acquisition

Initial measurements showed significant heating of the instrumented model pile, which resulted in large deviations in the strain gauge output voltage  $V_{output}$ . This was the result of a reasonable low strain gauge resistance combined with a small heat dissipation area. Installing a switched strain gauge bridge supply successfully resolved the heating issues. The resulting output voltage  $V_{output}$  was subsequently processed to retrieve the valid measurements at the 6V excitation level. The electric circuit, which was installed into a cable connected to the data acquisition system, consisted of a Diodes Inc ZXMP6A17G electronic switch, connected to a National Semiconductor LM555 timer.

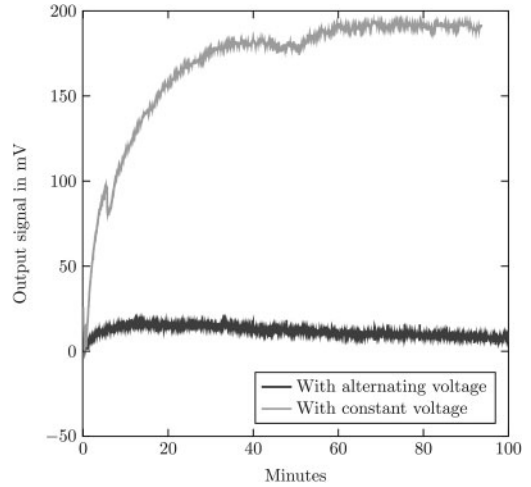


Figure 5. Effect of alternating bridge supply on thermal drift.

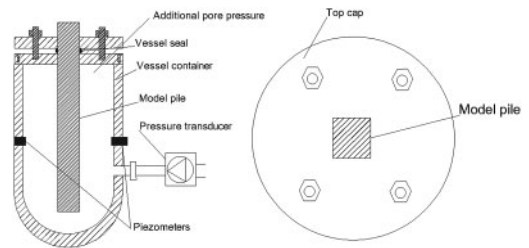


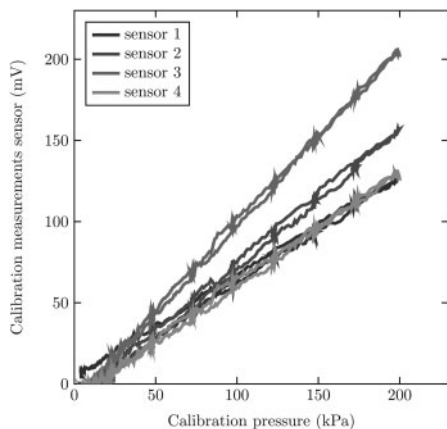
Figure 6. Vessel for the calibration of the horizontal stress gauges.

The duty cycle was 9% at 1.3 Hz frequency. Figure 5 shows the effectiveness of the system by plotting the evolution of  $V_{output}$  in time with and without the switched voltage regulation system.

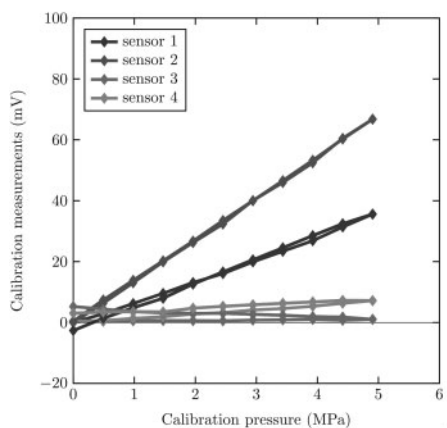
## 4 CALIBRATION

### 4.1 Procedure

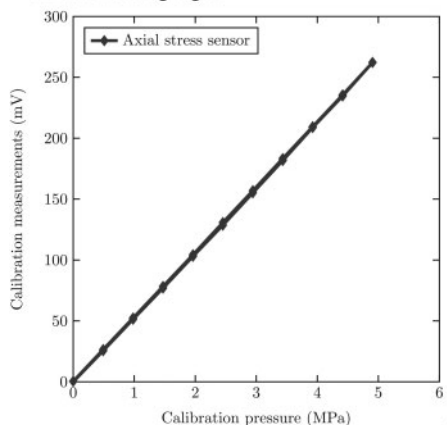
The instrumentation of the pile required a separate calibration procedure for the horizontal contact stress sensors and axial stress sensor. The horizontal contact stress sensor system was calibrated in a pressure vessel, providing an isotropic pressure at the stress sensor locations, shown in Figure 6. This vessel facilitates the calibration of the sensor without application of a pressure on the unsealed backside of the membrane via the pile head. The calibration vessel was sealed with a novel double layer cap top, in which a Teflon seal between model pile and the cap plates ensured a water tight seal upon compression in-between the top plates. A GDS standard pressure transducer controlled the pressure in the vessel. This vessel was equipped with two Druck PDCR-81 pore pressure transducers as a benchmark reading. During calibration the isotropic



(a) Contact stress gauges.



(b) Influence axial load on calibration of contact stress gauge.



(c) Base load.

Figure 7. Calibration results for the horizontal stress gauges and pile base sensor.

pressure in the vessel was incremented with steps of 25 kPa up to 200 kPa and subsequently incrementally unloaded. The calibration was repeated four times to assess the stability and consistency of the system. The

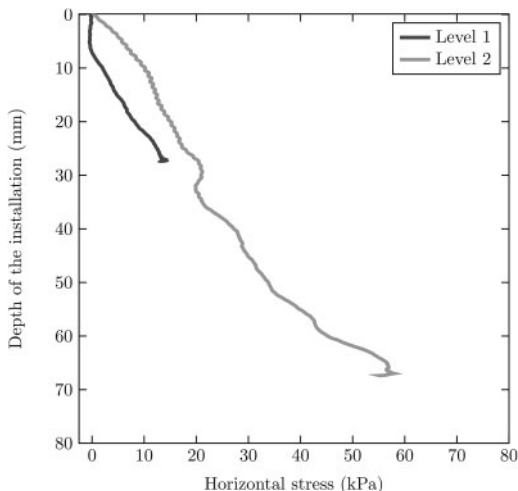


Figure 8. Pile installation test at 50-g using the newly developed model pile.

axial calibration was carried out with a lever system. The instrumented model pile was placed on a small steel sphere inserted into a drilled hole into the short end of the 5:1 lever for a moment-free load application. The vertical position of the model pile was adjusted for a horizontal lever position using a water level. During calibration the model pile was loaded to 5 MPa in 0.5 MPa increments, and then unloaded in 0.5 MPa increments.

## 4.2 Results

A representative loading-unloading calibration loop in the pressure vessel for the horizontal contact stress sensors and for the calibration of the axial stress sensor using the lever system is shown in Figure 7. Additionally, Figure 7 shows the influence on the horizontal contact transducers from the axial load in the pile. The sensor oscillations at constant pressure level are the result from small pressure variations caused by minor leaks in the vessel and subsequent crude regulation of the GDS controller.

## 5 DEMONSTRATION TEST

The instrumented model pile was tested in a loose silica sand sample at 50-g acceleration level at the TU Delft centrifuge (Allersma 1994). Measurements of the upper and lower instrumentation levels are shown for continuous installation in Figure 8. The measurements were carried out through the same measurement setup as used for the calibration, and the installation test show a steadily increasing horizontal contact stress with some reduction for the higher level, confirming measurements reported by (Lehane et al. 1993, Jardine et al. 2013).

## 6 CONCLUSIONS

An instrumented model pile for axial and horizontal contact stress measurements and a complementary calibration system have been realized. A novel electric mechanical arrangement of the sensor compensates for all negative influence of the axial load in the horizontal contact stress readings. The additional bending of the membrane resulting from axial load, however, remains. The latter is compensated using extensive cross-calibration as well as numerical analysis of the system. The model pile is successfully tested in a physical model test performed in the TU Delft Geotechnical centrifuge.

## ACKNOWLEDGMENTS

The research was funded by STW project number 10189. The support is gratefully acknowledged. The authors would like to thank Kees van Beek, Han de Visser and Ron van Leeuwen for their very kind and helpful assistance.

## REFERENCES

- Allersma, H. (1994). The university of delft geotechnical centrifuge. In *Proceedings International Conference Centrifuge 94*, pp. 47–52.
- Boulon, M. & P. Foray (1986). Physical and numerical simulation of lateral shaft friction along offshore piles in sand. In *Proceedings of the 3rd International Conference on Numerical methods in Offshore piling, Nantes, France*, pp. 127–147.
- Comsol (2008). Comsol multiphysics reference manual.
- El Ganainy, H., A. Tessari, T. Abdoun, & I. Sasanakul (2013). Tactile pressure sensors in centrifuge testing. *Geotechnical testing journal* 37(1), 151–163.
- Foray, P., J. Colliat, & J. Nauroy (1993). Bearing capacity of driven model piles in dense sands from calibration chamber tests. In *Offshore Technology Conference*, pp. OTC-7194-MS. Offshore Technology Conference.
- Garnier, J., C. Gaudin, S. M. Springman, P. J. Culligan, D. J. Goodings, D. Konig, B. Kutter, R. Philips, M. Randolph, & L. Thorel (2007). Catalogue of scaling laws and similitude questions in geotechnical centrifuge modelling. *International Journal of Physical Modelling in Geotechnics* 7(3), 1–23.
- Jardine, R., B. Lehane, & S. Everton (1993). Friction coefficients for piles in sands and silts. In *Offshore site investigation and foundation behaviour*, pp. 661–677. Springer.
- Jardine, R., B. Zhu, P. Foray, & Z. Yang (2013). Interpretation of stress measurements made around closed-ended displacement piles in sand. *Géotechnique* 63(8), 613–627.
- Klotz, E. & M. Coop (2001). An investigation of the effect of soil state on the capacity of driven piles in sands. *Géotechnique* 51(9), 733–751.
- Lehane, B., R. Jardine, A. Bond, & R. Frank (1993). Mechanisms of shaft friction in sand from instrumented pile tests. *Journal of Geotechnical Engineering* 119(1), 19–35.
- Poulos, H. G. & E. H. Davis (1980). *Pile foundation analysis and design*. Number Monograph.
- Randolph, M., R. Dolwin, & R. Beck (1994). Design of driven piles in sand. *Géotechnique* 44(3), 427–448.
- Reddy, J. N. (2006). *Theory and analysis of elastic plates and shells*. CRC press.
- Stuedlein, A. W. & T. N. Gianella (2016). Effects of driving sequence and spacing on displacement-pile capacity. *Journal of Geotechnical and Geoenvironmental Engineering* 143(3), 06016026.
- Talesnick, M., M. Ringel, & R. Avraham (2014). Measurement of contact soil pressure in physical modelling of soil–structure interaction. *International Journal of Physical Modelling in Geotechnics* 14(1), 3–12.